

Research article

Open Access

Oxidative stress causes ERK phosphorylation and cell death in cultured retinal pigment epithelium: Prevention of cell death by AG126 and 15-deoxy-delta 12, 14-PGJ₂

Tarun K Garg¹ and Jason Y Chang*^{1,2}

Address: ¹Departments of Anatomy & Neurobiology University of Arkansas for Medical Sciences Little Rock, AR 72205, USA and ²Ophthalmology University of Arkansas for Medical Sciences Little Rock, AR 72205, USA

Email: Tarun K Garg - gargtarunk@uams.edu; Jason Y Chang* - changjasony@uams.edu

* Corresponding author

Published: 21 March 2003

Received: 25 September 2002

BMC Ophthalmology 2003, 3:5

Accepted: 21 March 2003

This article is available from: <http://www.biomedcentral.com/1471-2415/3/5>

© 2003 Garg and Chang; licensee BioMed Central Ltd. This is an Open Access article: verbatim copying and redistribution of this article are permitted in all media for any purpose, provided this notice is preserved along with the article's original URL.

Abstract

Background: The retina, which is exposed to both sunlight and very high levels of oxygen, is exceptionally rich in polyunsaturated fatty acids, which makes it a favorable environment for the generation of reactive oxygen species. The cytotoxic effects of hydrogen peroxide (H₂O₂) induced oxidative stress on retinal pigment epithelium were characterized in this study.

Methods: The MTT cell viability assay, Texas-Red phalloidin staining, immunohistochemistry and Western blot analysis were used to assess the effects of oxidative stress on primary human retinal pigment epithelial cell cultures and the ARPE-19 cell line.

Results: The treatment of retinal pigment epithelial cells with H₂O₂ caused a dose-dependent decrease of cellular viability, which was preceded by a significant cytoskeletal rearrangement, activation of the Extracellular signal-Regulated Kinase, lipid peroxidation and nuclear condensation. This cell death was prevented partially by the prostaglandin derivative, 15d-PGJ₂ and by the protein kinase inhibitor, AG126.

Conclusion: 15d-PGJ₂ and AG126 may be useful pharmacological tools in the future capable of preventing oxidative stress induced RPE cell death in human ocular diseases.

Background

The retina, which is exposed to both sunlight and very high levels of oxygen, is exceptionally rich in polyunsaturated fatty acids, which makes it a favorable environment for the generation of reactive oxygen species. For example, retinal pigment epithelium (RPE) generates a number of reactive oxygen species when illuminated with light [1]. Furthermore, phagocytosis of photoreceptor outer segments by RPE causes an increase in intracellular [2] and extracellular H₂O₂ generation [3]. Oxidative stress has been suggested as the cause of a number of retinal pathological conditions [4,5].

A number of *in vitro* studies have attempted to characterize the effect of oxidative stress on RPE. Depending on the experimental conditions, treatment of RPE with H₂O₂ can cause an alteration of cellular functions [6,7] or cell death [8,9]. Cytotoxic levels of H₂O₂ can cause significant mitochondrial [10] and genomic [11] DNA damage in RPE simulating the features of programmed cell death [8,12]. Studies from other cell types indicate that early cellular events following H₂O₂ treatment include morphological alterations and actin re-organization [13]. In addition, activation of the ERK (p42/44, Extracellular signal-Regulated Kinase) MAP kinases (Mitogen-Activated Protein

kinases) can occur within minutes following cellular oxidative stress. Depending on the cell type examined, inhibition of the ERK activity can either prevent [14] or enhance H₂O₂-induced cell death [15]. The involvement of actin re-organization and ERK activation has not been examined in RPE under oxidative stress.

Lipid peroxidation products, such as 4-hydroxynonenal (4-HNE), have attracted considerable attention because of their potential involvement in aging and in a number of neuropathological conditions [16]. 4-HNE was implicated in the etiology of some pathological conditions in the eye. For example, levels of 4-HNE increased significantly in the vitreous of patients with proliferative vitreoretinopathy compared with controls [17]. Further, 4-HNE forms a stable adduct with rhodopsin in the photoreceptor, which may interfere with its functions [18]. 4-HNE even causes cataracts in cultured rat lens [19,20]. Whether oxidative stress on RPE can cause accumulation of cellular HNE-protein adducts remains unknown.

Peroxisome proliferator-activated receptors (PPARs) belong to a group of nuclear receptors that include steroid, retinoid, thyroid hormone receptors and others [21–23]. There are three types of PPARs: PPAR α is expressed predominantly in the liver, heart, kidney, brown adipose and stomach mucosa, and is important for lipid catabolism. PPAR γ is found in adipose tissues and is important for adipogenesis. PPAR β is found in most tissues, but its role is less well defined. RPE cells express all three forms of PPARs but PPAR β is the dominant isoform [24]. There is a 10-fold induction of PPAR γ mRNA that reaches a peak at 4-hour after phagocytosis of photoreceptor outer segments. The levels of either PPAR α mRNA or PPAR β mRNA are not altered under the same conditions. Increases in PPAR γ in RPE cells may be important for handling the lipids generated during the phagocytosis of photoreceptor outer segments [24]. Since RPE cells generate large amounts of H₂O₂ during the phagocytosis of photoreceptor outer segments, there is a possibility that activation of PPAR γ may assist in defending the oxidative stress associated with phagocytosis.

This study was designed to examine morphological alterations in RPE during oxidative stress, the involvement of ERK MAP kinase and 4-HNE and to test the hypothesis that PPAR γ activation can prevent oxidative damage on RPE cells. The human RPE cell line, ARPE-19, and primary cultures of adult human RPE were used in this study. ARPE-19 is a spontaneous occurring, non-transformed RPE cell line which expresses RPE specific markers (such as CRALBP and RPE65) and exhibits morphological polarization and tight junctions similar to native RPE [25,26].

Methods

Materials

WY14643, 15d-PGJ₂, azelaoyl PAF and ciglitazone were purchased from Cayman (Ann Arbor, MI). LY 171883 was purchased from Alexis Biochemicals (San Diego, CA). AG126 and PD98059 were purchased from Calbiochem (San Diego, CA). Hydrogen peroxide and other pharmacological and general biochemical reagents were purchased from Sigma (St. Louis, MO) unless otherwise stated.

Cell cultures

ARPE-19 cells [25] were obtained from the American Type Culture Collection and grown in DMEM/F12 containing 10% heat-inactivated fetal bovine serum and 2.5 mM glutamine. Human primary RPE cultures were established from donor eyes obtained from the Arkansas Lions Eye Bank & Laboratory. The globe was sectioned at the ora serrata, and the lens and vitreous body were removed. The eye cup was then filled with 4% dispase (prepared in DMEM) containing 1 \times antibiotic-antimycotic reagents (final concentrations: 100 units/ml Penicillin G, 100 μ g/ml Streptomycin and 0.25 μ g/ml Amphotericin B) and incubated in a 37°C incubator with 5% CO₂ for ~30 minutes. RPE cells were then removed under a dissecting microscope, dissociated by trituration using a Pasteur pipette, and then plated on poly-L-lysine (25 mg/liter in water) coated 35-cm² culture dishes. The cell population was then expanded by sequentially subculturing into 25-cm² tissue culture flasks, then to 75-cm² tissue culture flasks. Cells of passages #3–#6 were used for this study. The culture medium consisted of 10% heat-inactivated fetal bovine serum, 2.5 mM glutamine and 1 \times antibiotic-antimycotic reagents in DMEM.

Cell viability

Cells were plated in 96-well plates (human primary RPE: 10,000 cells/well, ARPE-19: 15,000–20,000 cells/well, unless otherwise stated) overnight, fed with serum-free medium or treated with testing agents (prepared in serum-free medium) the next day followed by H₂O₂ treatment for a day, then the viability from each treatment was determined by the MTT (3-(4,5-dimethylthiazol-2-yl)-2,5-diphenyltetrazolium bromide) assay [27]. Culture medium was removed after treatment and then 100 μ l MTT solution (100 μ g/ml prepared in DMEM) was added to each well. The cultures were incubated at 37°C for one hour in a tissue culture incubator. The MTT solution was then removed and the cells in each well were lysed by the addition of 100 μ l dimethyl sulfoxide. The plate was placed on a shaker for one hour at room temperature to complete the lysing process, then the optical density of each well was measured by a 96-well plate reader with a filter setting at 570 nm (reference filter setting was 630 nm). When a pharmacological agent was used in the

experiment, the MTT reading from cultures treated with that agent alone was used as 100% cellular viability.

Actin staining

This was performed as described by Carter et al. [28]. Cells grown on coverslips were treated with H₂O₂ for various period of time as indicated in figure legends, washed three times with phosphate-buffered saline (PBS), then fixed for 10 minutes with 3.7% formaldehyde (prepared in PBS). The cultures were then washed three times with PBS, extracted with -20°C acetone for 5 minutes followed by three washes with PBS. Each culture was then stained with Texas Red-phalloidin (Molecular Probes, Eugene, OR) prepared in PBS containing 1% bovine serum albumin for 20 minutes at room temperature in a lightproof box. The cultures were then washed three times with water, mounted with GEL/MOUNT (Biomedica, Foster City, CA). The slides were examined under a Nikon microscope Eclipse E600 (Nikon Instruments Inc., Melville, NY). Cells were photographed digitally at a fixed exposure time by using a Photometrics CoolSNAP fx camera (Roper Scientific, Inc., Tucson, AZ) and the software MetaVue, Meta Imaging Series 4.5 (Universal Imaging Corporation, Downingtown, PA).

Immunohistochemical and immunofluorescent staining

Cultures grown on coverslips were used in this set of experiments. Phospho-ERK was detected by mouse anti-phospho-ERK antibody (Santa Cruz Biotechnology, Santa Cruz, CA, used at 1:1500) and the Vectastain ABC kit (Vector Lab., Burlingame, CA) with diaminobenzidine as the chromogen. Cellular 4-HNE protein adducts were detected by rabbit anti-4-HNE antibodies (Calbiochem, San Diego, CA, used at 1:250) followed by anti-rabbit secondary antibody labeled with FITC (Dako Corporation, Carpinteria, CA). The cultures were then mounted with GEL/MOUNT. The slides were examined under Nikon microscope Eclipse E600 (Nikon Instruments Inc., Melville, NY). Cells were photographed at fixed exposure time with Nikon digital still camera DXM 1200 (Nikon Instruments Inc., Melville, NY) and the software Nikon ACT-1 version 2.11 (Nikon Corporation, Tokyo, Japan).

Nuclear staining

Cells grown on coverslips were treated with H₂O₂ for various periods of time as indicated in figure legends, fixed for 10 minutes with 3.7% formaldehyde (prepared in PBS), stained with 1 µg/ml bisbenzimidazole solution (Hoechst 33258, Sigma, St. Louis, MO) for 10 minutes at room temperature, mounted with GEL/MOUNT, then observed under a fluorescent microscope as described in the previous section.

Western blot analysis

RPE cells were plated in T-150 flasks overnight, fed with serum-free medium for a day, then treated with H₂O₂ as indicated in figure legends. For sample preparation, cultures were detached with a scraper in PBS then centrifuged. The cell pellets were suspended in 150–300 µl ice-cold RIPA lysis buffer (1% NP-40, 0.5% Na-deoxycholate, 0.1% SDS in PBS, 0.5 mM Phenylmethylsulfonyl fluoride (PMSF), 0.02 mg/ml Aprotinin, 1 mM Na₃VO₄) and incubated for 30 min on ice. Each sample was further homogenized by passage through a 21-gauge needle followed by an addition of 10 µl PMSF (stock solution: 50 mM). The samples were then incubated for 30 min on ice and subsequently centrifuged at 14,000 RPM for 20 min at 4°C. The supernatant from each sample was collected and an aliquot was taken for protein concentration determination by Micro BCA Protein Assay Reagent Kit (Pierce, Rockford, IL). Protein samples were stored at -70°C until ready for electrophoretic analysis. Equal amounts of protein samples (20 µg/well) were heated at 95°C for 6 min then loaded onto 1% SDS, 10% polyacrylamide gels. BenchMark pre-stained protein ladder (Invitrogen life technologies, Carlsbad, California) was used as molecular weight standards. Following electrophoretic separation, the proteins were transferred to nitrocellulose membranes. Equal loading and appropriate transfer of each lane was confirmed by staining the membrane with the Ponceau S solution (Sigma, St. Louis, MO). Membranes were blocked in 5% nonfat dried milk for one hour, washed in 10 mM Tris-buffered saline (pH 7.5) containing 0.1% Tween-20 (TBST) and probed with primary antibody overnight at 4°C. Membranes were washed with TBST and then incubated for 1 hour at room temperature with a secondary antibody followed by washing three times with TBST, immersed in ECL Plus western blotting detection system (Amersham Pharmacia Biotech, Buckinghamshire, England) for 1 min and then exposed to Kodak X-ray film (Rochester, NY). The films were analyzed by densitometry using a ChemImager 5500 imaging system with AlphaEaseFC software (Alpha Innotech Corporation, San Leandro, CA). Results, expressed as percentage of control, from replicate experiments were pooled and averaged. The primary antibodies used in this set of experiments were from Santa Cruz (anti-ERK 1/2, used at 1:5000; anti-phospho-ERK, used at 1:1000; anti-PPAR γ , used at 1:2000) or from Calbiochem (anti-4-HNE, used at 1:2,000).

Statistical analysis

Unless otherwise stated, results of cell viability experiments were pooled from 12 replicate samples derived from 3 independent experiments, and expressed as mean \pm SEM. Statistical analyses were performed by analysis of variance (one-way ANOVA) followed by the Bonferroni test to determine the significance of difference.

Results

Cytotoxicity of H₂O₂ toward primary human RPE and ARPE-19 cells

Initial experiments analyzing the cytotoxic effect of oxidative stress on primary cultures of human RPE cells indicated that H₂O₂ at 1 mM or less did not affect cellular viability. Higher concentrations caused a sharp decrease of viability in human RPE such that a 24-hour treatment of cells with 1.2 mM H₂O₂ lowered the viability to 13% of controls (Fig. 1A, squares). This concentration lowered the viability of human RPE to 62% after a 4-hour treatment (Fig. 1A, circles).

In a set of analogous experiments, ARPE-19 cells treated with various concentrations of H₂O₂ for 4 hours or 24 hours showed that a 4-hour treatment with 1 mM H₂O₂ did not affect viability. An increase of H₂O₂ concentrations beyond 1 mM decreased viability such as 2 mM H₂O₂ decreased the viability to 46% of controls in 4 hours (Fig. 1B, circles). Treatment of cells with H₂O₂ for 24 hours caused a dose-dependent decrease of viability with a LD₅₀ of ~1.35 mM (Fig. 1B, squares).

H₂O₂ induced cytotoxicity in RPE cells appears to be affected by the density of cells in cultures [29]. To study this phenomenon, ARPE-19 cells plated in 96-well plates with densities of 10,000, 20,000 or 40,000 cells/well were subjected to H₂O₂ treatment. Cells grown in a high-density culture were indeed more resistant to H₂O₂ as compared to those grown in a low-density culture (Fig. 1C). For example, H₂O₂ at 1.4 mM reduced cellular viability to 11%, 49% or 94% of control in cultures with 10,000, 20,000 or 40,000 cells/well, respectively.

H₂O₂ induced morphological alterations and formation of 4-HNE-adducts

To analyze morphological changes of RPE cells treated with a cytotoxic concentration of H₂O₂, ARPE-19 cells were treated with 1.5 mM H₂O₂ for various periods of time and then processed for actin staining. Without H₂O₂ treatment, stress fibers appeared thin and diffuse in control cells (Fig. 2A, arrow). At 15-min after treatment, these cells appeared to round up and significant ruffling occurred at the edge of their plasma membrane (Fig. 2B, arrows). Overall thickening of stress fibers occurred at two hours after treatment in addition to the membrane ruffling (Fig. 2C, arrows). Additional morphological changes after 4 hours of H₂O₂ treatment (Fig. 2D,2E,2F) included distinctive dense bands at the periphery of some cells (Fig. 2D, arrows), peri-nuclear staining of actin fibers in other cells (which made the nuclei prominent, Fig. 2E, arrows) and microspikes (Fig. 2F, arrow) on the cell surface of some cells.

Subsequent experiments with immunofluorescent staining indicated that 1.5 mM H₂O₂ treatment of ARPE-19 cells for 4 hours led to the formation of 4-HNE protein adducts both in the cytoplasm and nucleus, presumably as a result of lipid-peroxidation (Fig. 3A,3B). Various protein bands on Western blots were positive for anti-HNE antibody reactivity, further intensified as a result of H₂O₂ treatment (Fig. 3C). Densitometry measurements were performed to estimate the collective increase of band intensity in each lane between 39 Kd and 87 Kd. Results derived from a total of six independent experiments indicated that treatment of cells with 0.5, 1, 1.5 or 2 mM H₂O₂ caused an increase of intensity to 2.5-, 3.1-, 3.7- or 7.1-fold of control, respectively.

Though there was significant cytoskeletal alterations and lipid peroxidation at 4 hours after H₂O₂ treatment, nuclear staining using bisbenzimidazole (Hoechst 33258) indicated that most cells maintained normal nuclear morphology at this time (Fig. 4A, untreated cells; Fig. 4B, 4 hours after treatment). Nuclear condensation increased with length of H₂O₂ exposure, which was clearly evident at 12 hours after H₂O₂ treatment (Fig. 4C, arrows), and even more prominent at 16 hours after treatment (Fig. 4D). These results suggest that H₂O₂ treatment caused apoptosis in RPE. Nuclear condensation appeared to start at the edge of the culture (relatively lower density area, Fig. 4C, arrows) and spread to the center part of the culture (higher density, Fig. 4D) over time. This phenomenon is consistent with the viability assay in which higher density cultures were more resistant to oxidative stress (Fig. 1C).

Effect of oxidative stress on PPAR γ protein expression

During rod outer segment ingestion, there is a generation of H₂O₂ [2,3] and an up-regulation of PPAR γ mRNA expression [24] in RPE, experiments were performed to determine if H₂O₂ could induce PPAR γ protein expression over the control levels. ARPE-19 cells were treated with various concentrations (0.5, 1, 1.5, 2 mM) of H₂O₂ for 24 hours and processed for Western blot analysis. Results indicated a slight induction of PPAR γ protein levels in some experiments. This induction, however, was not apparent in other experiments (Results not shown). Densitometry analyses from a total of six independent experiments indicated that treatment of these cells with 0.5, 1, 1.5 or 2 mM H₂O₂ for 24 hours caused an alteration of band intensity to 76%, 108%, 113% or 104% of controls, respectively. There was no significant change of PPAR γ protein level after 30-min or 12-hour H₂O₂ treatment, either (results not shown). A separate set of experiments also indicated that treatment of primary human RPE cells with 1 mM H₂O₂ for 24 hours did not induce PPAR γ protein expression over the control levels (results not shown).

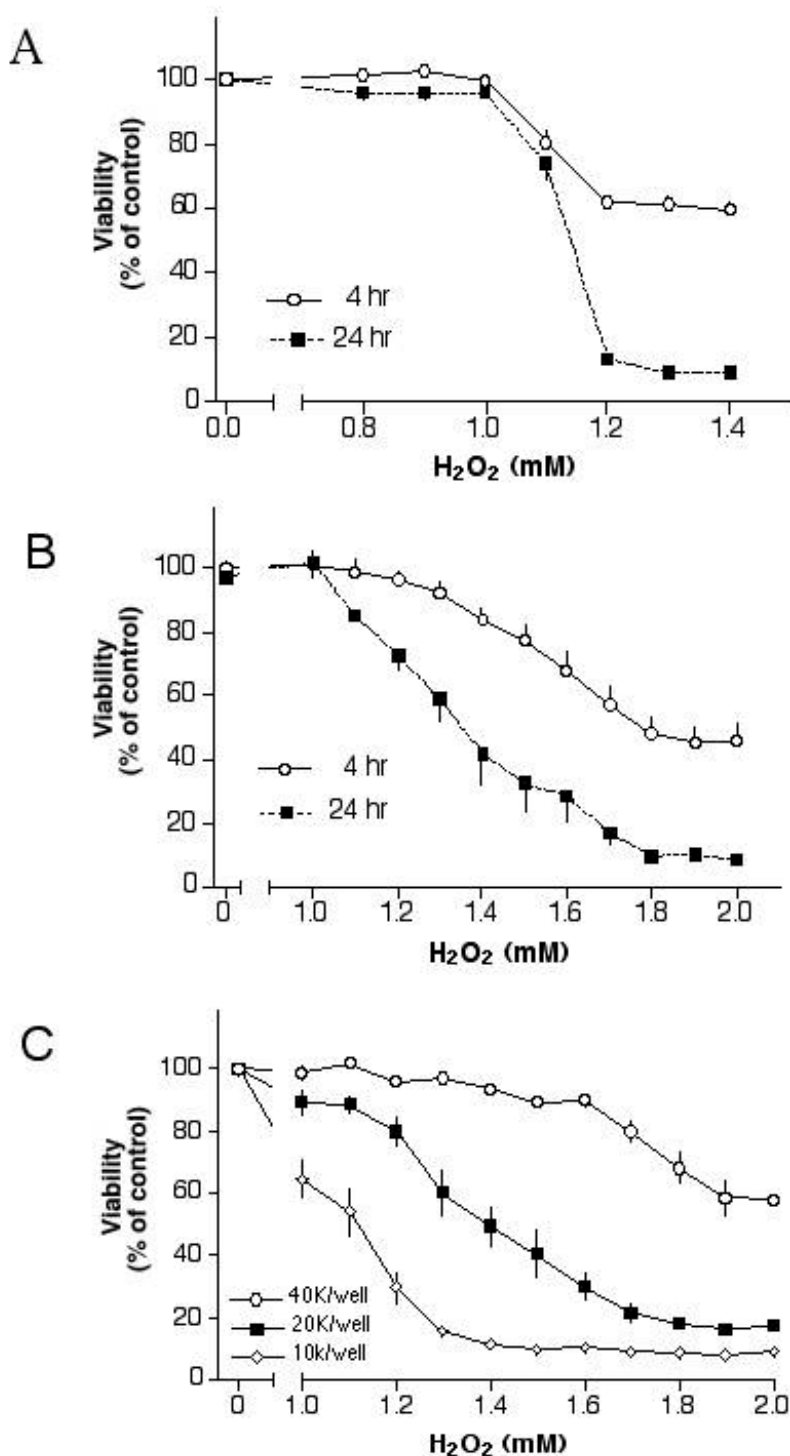


Figure 1

Cytotoxicity of H₂O₂ on human RPE cells. Fig. 1A: Primary human RPE cells were plated in 96-well plate, fed with serum-free medium the next day, then treated with H₂O₂ for 4 hours (circles) or 24 hours (squares). Fig. 1B: ARPE-19 cells were plated in 96-well plate, fed with serum-free medium the next day, then treated with H₂O₂ for 4 hours (circles) or 24 hours (squares). Fig. 1C: ARPE-19 cells were plated with a density of 10,000 cells/well, 20,000 cells/well or 40,000 cells/well in 96-well plates, fed with serum-free medium the next day, then treated with H₂O₂ for 24 hours. The viability of each treatment was determined by the MTT assay. Cultures at a density of 40,000 cells/well were 100% confluent.

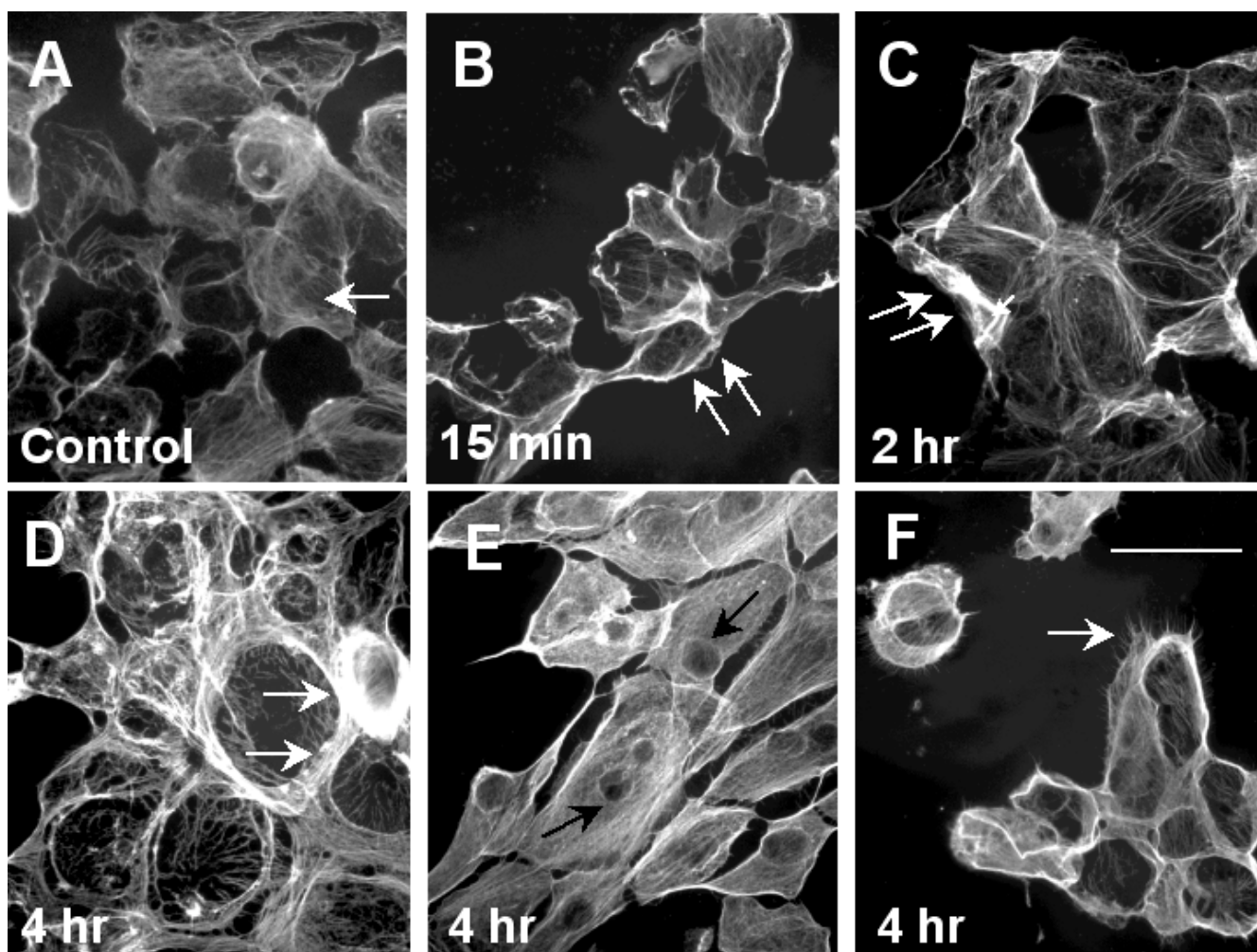


Figure 2

Reorganization of actin fibers caused by oxidative stress. ARPE-19 cells were treated with 1.5 mM H_2O_2 then processed for actin stain as described in the Methods. Fig. 2A: untreated; Fig. 2B: 15-min; Fig. 2C: 2-hour; Figs. 2D,2E and 2F: 4-hour after treatment. See text for detailed discussion of the results. Scale bar in Fig. 2F: 50 μ m.

Prevention of oxidative stress induced cytotoxicity by $PPAR\gamma$ agonists

Even though H_2O_2 did not increase $PPAR\gamma$ protein expression significantly as indicated in the previous study, experiments were performed to determine whether $PPAR\gamma$ agonists could activate the existing $PPAR\gamma$ thus preventing H_2O_2 induced cytotoxicity in RPE cells. Cells were pretreated with the $PPAR\gamma$ agonist 15d-PGJ₂ overnight followed by H_2O_2 for one day (without 15d-PGJ₂) and processed for the MTT viability assay. Results indicated that 15d-PGJ₂ prevented H_2O_2 induced cytotoxicity in primary human RPE cultures in a dose-dependent manner (Fig. 5A). Subsequent experiments with ARPE-19 cells also indicated this saving effect. While H_2O_2 at 1.3 mM, 1.4 mM or 1.5 mM lowered the ARPE-19 viability to 64%,

46% or 28% of control, respectively; pretreatment of these cells with 1 μ M 15d-PGJ₂ raised the viabilities to 95%, 84% or 68% of control, respectively (Fig. 5B). Cells stained with Hoechst 33258 indicated that 15d-PGJ₂ prevented H_2O_2 induced nuclear condensation (Fig. 4E; compare this with Fig. 4D). The other $PPAR\gamma$ agonists, ciglitazone [30], azelaoyl PAF [31] and LY171883 [32], however, were not effective (tested between 1–10 μ M, 3 independent experiments for each agent, results not shown). The $PPAR\alpha$ agonist WY14643 had some saving effect at a high concentration (40 μ M), however, the difference was not statistically significant (results not shown).

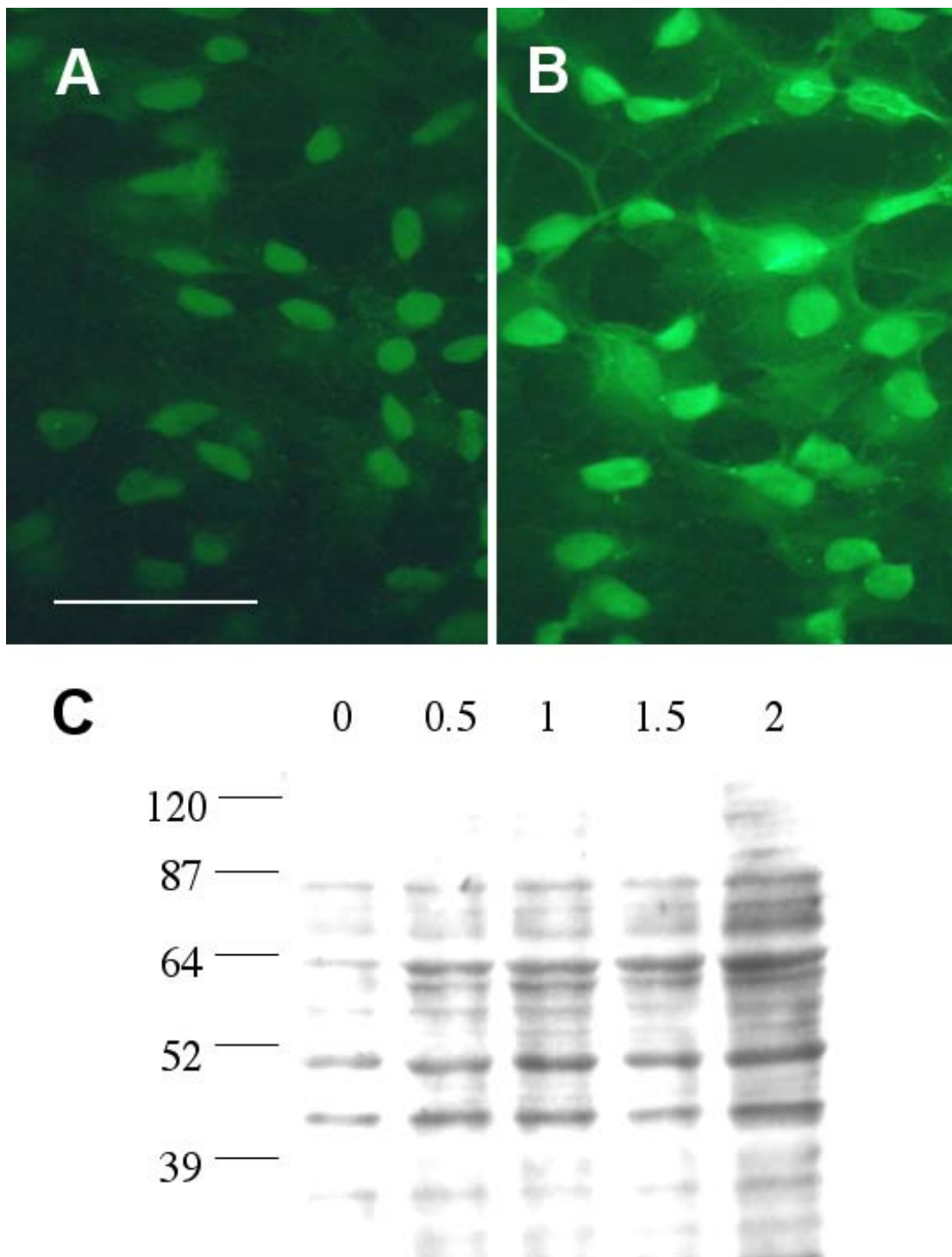
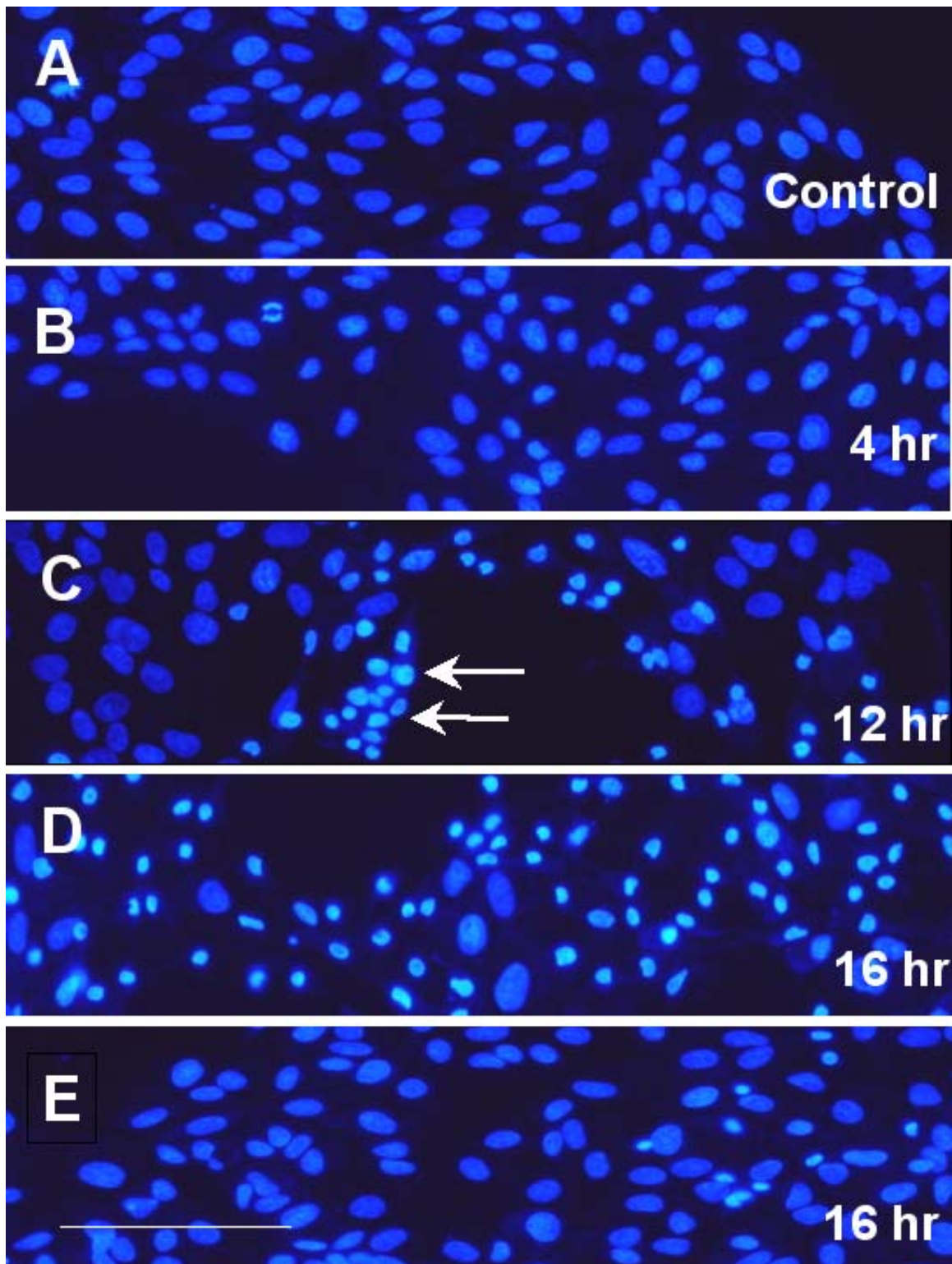


Figure 3

H₂O₂ induced lipid peroxidation in RPE. ARPE-19 cells were treated with 1.5 mM H₂O₂ for 4 hours then processed for immunofluorescent staining using antibodies against 4-HNE. Fig. 3A: untreated cells. Scale bar: 50 μm. Fig. 3B: H₂O₂ treated cells. Note the overall enhanced staining in nucleus and cytoplasm. Fig. 3C: ARPE-19 cells were treated with various concentrations (0.5, 1, 1.5, 2 mM) of H₂O₂ for 24 hours then processed for Western blot analysis using anti-4-HNE antibodies. These polyclonal antibodies recognize cysteine-, histidine- and lysine-4-HNE Michael adducts. This is a representative result from 6 similar experiments.

**Figure 4**

H_2O_2 induced nuclear condensation in ARPE-19 cells. ARPE-19 cells were treated with 1.5 mM H_2O_2 for various periods of time, and then processed for nuclear staining. Fig. 4A: untreated cells; Fig. 4B: 4-hour; Fig. 4C: 12-hour; Fig. 4D: 16-hour after treatment. Fig. 4E: Cells were pretreated with 1 μ M 15d-PGJ₂ overnight, followed by 1.5 mM H_2O_2 for 16 hours (without 15d-PGJ₂). See text for detailed description of the results. Scale bar in Fig. 4E: 100 μ m.

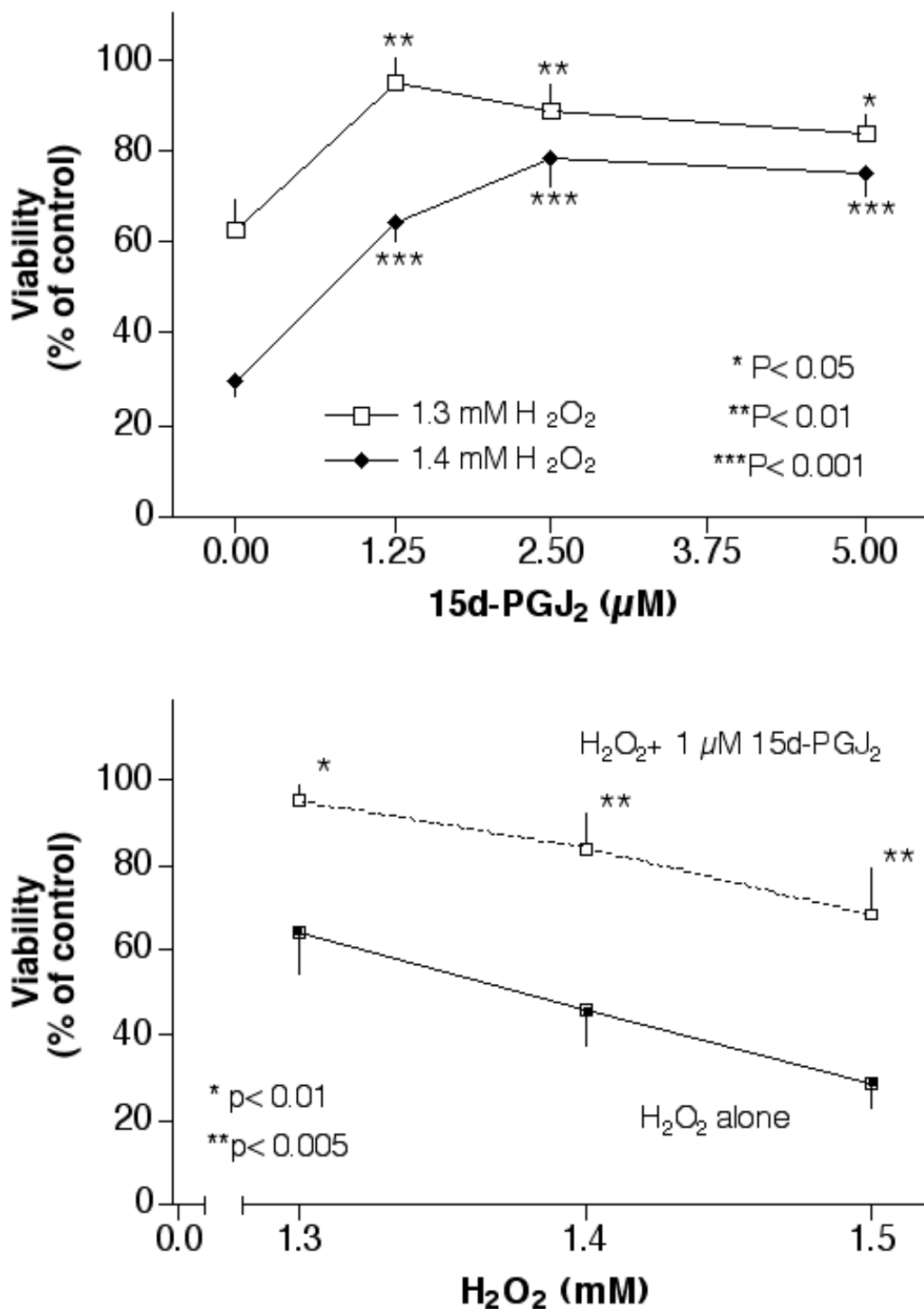


Figure 5

Prevention of H₂O₂ induced cytotoxicity by 15d-PGJ₂ in RPE cells. Fig. 5A: Primary RPE cells were pretreated with various concentrations of 15d-PGJ₂ overnight, followed by 1.3 mM or 1.4 mM H₂O₂ for 1 day (without 15d-PGJ₂), then processed for the MTT viability assay. Fig. 5B: ARPE-19 cells were pretreated with 1 μM 15d-PGJ₂ overnight, followed by various concentrations of H₂O₂ for 1 day (without 15d-PGJ₂), then processed for the MTT viability assay. Statistical analyses were performed comparing cells treated with H₂O₂ alone versus H₂O₂ plus 15d-PGJ₂.

Activation of ERK by H₂O₂

A set of experiments was performed to determine the effects of H₂O₂ on ERK activation. ARPE-19 cells were treated with 1.5 mM H₂O₂ for 1 hour and processed for immunohistochemical staining using antibodies against phospho-ERK. Untreated cells showed a faint phospho-ERK staining while there was an apparent increase of phospho-ERK staining in the cytoplasm and nuclei in H₂O₂ treated cells (Fig. 6A,6B). A separate set of cultures was treated with H₂O₂ for 30 min and then processed for Western blot analysis. This H₂O₂ treatment of the cells caused only a slight alteration in ERK levels but led to a dose-dependent increase of phospho-ERK, with a maximal stimulation observed at 1.5 mM (Fig. 6C). Densitometry analyses from 3 independent experiments indicated that 0.5, 1, 1.5 or 2 mM H₂O₂ caused an increase of p42ERK (ERK2) phosphorylation to 2.1-, 12.7-, 18.8- or 2.0- fold of control, respectively. Similar treatment caused an increase of p44 ERK (ERK1) phosphorylation to 1.5-, 15.7-, 21.4- or 3.4-fold of control, respectively. The phospho-ERK in H₂O₂ treated samples remained higher than control at 24-hour after treatment (results not shown).

Effect of ERK inhibition on H₂O₂ induced cytotoxicity in ARPE-19

Since ERK activation appeared to be an early event associated with H₂O₂ induced cytotoxicity, experiments were performed to determine if inhibitors of ERK activation could affect the cytotoxicity caused by H₂O₂. ARPE-19 cells were pretreated with 10 μM PD98059 (a MEK inhibitor which functions upstream of ERK [33]) followed by H₂O₂ challenge. Results from 3 independent experiments indicated that this agent could prevent low-dose (1–1.2 mM) H₂O₂ induced cell death slightly. In contrast, it enhanced high-dose (1.3–1.6 mM) H₂O₂ induced cell death. These effects in either case were not remarkable (results not shown). This agent at concentrations higher than 10 μM was toxic to ARPE-19 cells by itself and could enhance H₂O₂ toxicity (results not shown).

In a separate set of experiments, ARPE-19 cells were pretreated with 10 μM AG126 (a protein tyrosine kinase inhibitor [34]) followed by H₂O₂ challenge. The treatment of cells with 1.3 mM, 1.4 mM or 1.5 mM H₂O₂ decreased the cellular viability to 66%, 40% or 22% of control, respectively. Pretreatment of cells with AG126 raised the viability to 72% ($p < 0.05$ compared to H₂O₂ treatment only), 63% ($p < 0.005$) or 35% ($p < 0.01$) of control, respectively. AG126 at concentrations higher than 10 μM was toxic to ARPE-19 cells by itself and could enhance H₂O₂ toxicity (results not shown).

Both AG126 (10 μM) and 15d-PGJ₂ (1 μM) could prevent H₂O₂ induced cytotoxicity in ARPE-19, a set of experiments was also performed to determine whether these

two agents had additive saving effects. While 1.4 mM H₂O₂ treatment reduced the viability to ~40% of control, AG126 raised this viability to ~55% of control and 15d-PGJ₂ raised the viability to 75% of control. A combination of these two agents did not raise the viability above 15d-PGJ₂ alone (Fig. 7).

Discussion

Cytotoxicity of oxidative stress on RPE

Results from this study indicated that both primary human RPE cultures and ARPE-19 cells were susceptible to H₂O₂ treatment. It is important to point out that H₂O₂ showed a very steep dose-response curve in primary RPE cultures under our experimental conditions such that an increase of H₂O₂ concentration from 1 mM to 1.2 mM for one-day treatment caused a decrease in viability from ~100% to ~10% of control (Fig. 1A). Though the H₂O₂ titration curve in ARPE-19 was not as steep as observed in primary RPE, one-day treatment of these cells with 1.8 mM H₂O₂ could decrease the cellular viability to ~10% of control while 1 mM H₂O₂ did not affect cellular viability (Fig. 1B). The sharp dose-response curves demonstrated in this study suggests that it is important to have an effective cellular anti-oxidation mechanism to prevent the build-up of oxidative stress over a critical level. An increase of oxidative stress in RPE is associated with an increase of cellular catalase, metallothionein [3] and glutathione S-transferase [35], which should serve as a protective mechanism to decrease the cytotoxicity caused by H₂O₂ and other reactive oxygen species. This protective mechanism declines with age because a study analyzing metallothionein levels in RPE of macular region showed a dramatic decrease in aged donors (mean age = 80-yr) as compared to those from younger donors (mean age = 58-yr) [36]. A separate report concluded that there was also an age-dependent decrease of catalase activity in RPE [37]. These studies suggest RPE in the elderly are more susceptible to oxidative stress induced damage, which may contribute to age-related RPE dysfunction and vision loss. The oxidative stress induced RPE cytotoxicity can be aggravated by zinc deficiency, as previously reported by Tate et al. [9].

Significant morphological changes were observed in RPE cells treated with a cytotoxic concentration of H₂O₂. Actin fiber re-organization was noticed as early as 15 minutes after treatment (Fig. 2). Those images presented in Fig. 2D,2E and 2F are three representatives of RPE cells at 4 hr after H₂O₂ treatment. The cells shown in 2D and 2F are commonly seen at different locations on the same slide. In Fig. 2D, the dense peripheral bands of actin fibers were very prominent in some cells and the high intensity fluorescence caused an impression that the cells were relatively empty. The thickening of dense peripheral bands in this study was in contrast to previous

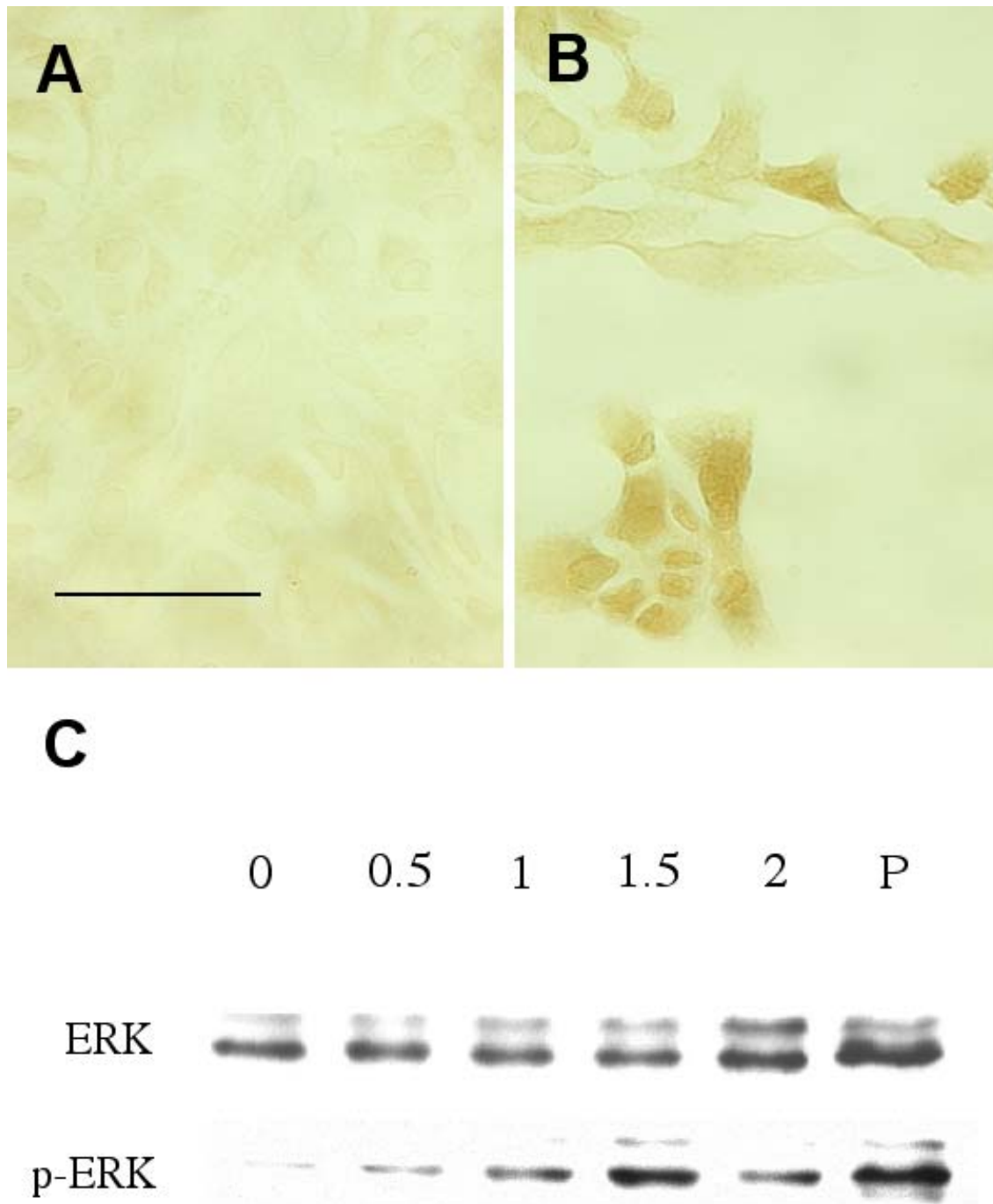


Figure 6

Activation of ERK by H₂O₂ treatment. ARPE-19 were treated with 1.5 mM H₂O₂ for one hour, then processed for immunohistochemical staining using anti-phospho-ERK antibody. Fig. 6A: untreated cells. Scale bar: 50 μm. Fig. 6B: H₂O₂ treated cells. Fig. 6C: ARPE-19 were treated with various concentrations (0.5, 1, 1.5, 2 mM) of H₂O₂ for 30 minutes, and then processed for Western blot analysis. Antibodies against ERK and phospho-ERK were used in this study. P: positive controls. This is a representative result from 3 similar experiments.

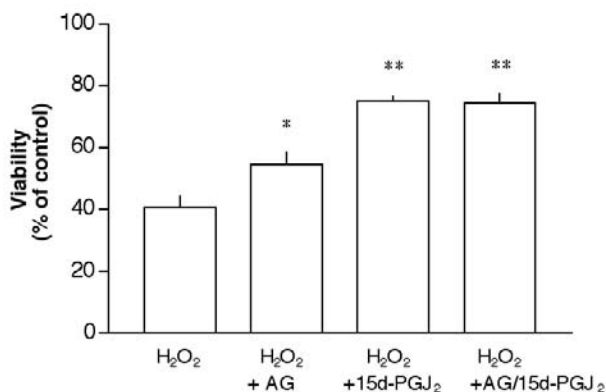


Figure 7

Saving of RPE cells by AG126 and 15d-PGJ₂. ARPE-19 cells were treated with 10 μM AG126, 1 μM 15d-PGJ₂ or a combination of these two agents overnight, followed by 1.4 mM H₂O₂ for 1 day (without testing agents), then processed for the MTT viability assay. *P < 0.05 as compared to H₂O₂ alone; **p < 0.001 as compared to H₂O₂ alone. There was no statistical difference between H₂O₂ + 15d-PGJ₂ and H₂O₂ + AG/15d-PGJ₂.

observations in endothelial cells. For example, Zhao and Davis reported that cultured pulmonary endothelial cells treated with H₂O₂ underwent a morphological change that was accompanied by an accumulation/increase in stress fibers running across the cells while the dense peripheral bands of most cells were disrupted or eliminated [38]. Similar observations on endothelial cells were made by Liu and Sundqvist [39]. The dense peripheral bands are important in cell-cell adhesion, which maintains the structural integrity. While it is apparent that endothelial cells used in those studies and epithelial cells used in this study respond differently to H₂O₂, the underlying reason for this difference is currently unknown. One may speculate that RPE cells use this build-in mechanism to defend the oxidative stress that they are constantly exposed to. We currently have no data to support or dismiss this possibility. In Fig. 2E, some cultures responded to H₂O₂ treatment by a perinuclear distribution of actin fibers. In Fig. 2F, we observed microspikes at the periphery of the cells. A detailed study of microspikes by Adams indicated that these structures consist of actin, the actin binding protein, 55 kd/fascin and myosin [40]. The perinuclear staining and microspikes of cells under oxidative stress in this study are very similar to those observed by Huot et al. in endothelial cells treated with H₂O₂ [41]. The functional significance of these structural changes in RPE after H₂O₂

treatment is not clear. There is a possibility that the appearance of microspikes around the cells under stressed conditions is an adapted behavior of the cells in order to attach to the substratum firmly. Prolonged H₂O₂ treatment led to cell death with the appearance of condensed nuclei is an indication of apoptosis (Fig. 4C,4D). This general finding is consistent with that observed by others [8,12].

It is of interest to note that cultures with a reduced density are more vulnerable to H₂O₂ treatment (Fig. 1C). One straightforward explanation for the vulnerability of low-density cultures treated with H₂O₂ is that more molecules of H₂O₂ per cell were present in these low-density cultures, which caused a lower viability. If this were the case, a mathematic analysis of the H₂O₂ molecules per cell should be able to estimate the cytotoxicity in this experimental system. For example, 1.4 mM H₂O₂ in a culture plated at a density of 40,000 cells/well should result in a viability close to twice of that generated in 20,000 cells/well and four times of that in 10,000 cells/well. Results from Fig. 1C indicated that the viability of each condition above was 94%, 49% or 11%, respectively. It is apparent that H₂O₂ killed more cells in cultures of lower density (10,000 cells/well) than expected. Because the result could not always be predicted by a mathematic estimation, there is a possibility that cell-cell contacts and some autocrine/paracrine production in a culture may alter the microenvironment thus determine the cytotoxicity caused by H₂O₂. Since cells with lower density are more susceptible to oxidative stress, there is a possibility that a vicious cycle exists such that when an area of RPE loses some of the constituent cells by oxidative stress, the remaining cells will become even more vulnerable to this insult.

PPARs in RPE

This study indicated that the PPARγ agonist 15d-PGJ₂ could prevent H₂O₂ induced RPE cell death (Figs. 5A,5B and Fig. 4E). This suggests that this agent can prevent oxidative stress induced RPE damage. This finding is significant given prior reports that oxidative stress on RPE is an important contributing factor of age-related macular degeneration [5,42]. An earlier report also indicated that PPARγ agonists could prevent laser photocoagulation induced choroidal neovascularization in rat eyes and monkey eyes, which suggests the possible application of these agents on the exudative form of age-related macular degeneration [43]. It is important to note that the other PPARγ agonists tested in this study (ciglitazone, azelaoyl PAF and LY171883) were ineffective in saving cells under the same experimental conditions. Since three out of four PPARγ agonists tested were ineffective, this raises the possibility that the saving effect of 15d-PGJ₂ is not through PPARγ activation. In this respect, it should be noted that

this agent has been shown to exert some biological effects that are independent of PPAR γ activation [44–46].

We have previously shown that 15d-PGJ $_2$ can prevent the cytotoxicity of cholesterol oxides, end products of cholesterol under oxidative stress [27]. Together with results from the current study, this agent may have a general protective effect against oxidative stress itself or against cytotoxic agents generated by oxidative stress. It is important to note that 15d-PGJ $_2$ functions as a general inhibitor of immune activities. For example, this agent is a potent inhibitor of microglia, the macrophage-like cells in the central nervous system [47–49] and shown to be effective in reducing the symptoms of experimental autoimmune encephalomyelitis (EAE), an animal model for the human disease multiple sclerosis [50]. Together, these results suggest that this agent may be useful in preventing ocular diseases that result from oxidative stress or inflammation.

ERK activation and 4-HNE protein adducts formation as a result of oxidative stress

Oxidative stress is a potent stimulator of the MAP kinase activities [14,15,51]. Phosphorylation of ERK could be observed within 30–60 minutes after H $_2$ O $_2$ treatment (Fig. 6). There are conflicting results in literature regarding whether an increase of ERK phosphorylation is beneficial or detrimental to cell survival. Bhat et al. demonstrated that 5–25 μ M PD98059 could prevent H $_2$ O $_2$ induced cell death in an oligodendrocyte cell line [14]. In contrast, 20 μ M PD98059 was shown to enhance cell death caused by H $_2$ O $_2$ treatment in HeLa cells [15]. This reagent had no significant effect on H $_2$ O $_2$ treated ARPE-19 cells under our experimental conditions. AG126, on the other hand, appeared to reduce the cytotoxicity caused by oxidative stress (Fig. 7). While this suggests that inhibition of tyrosine phosphorylation or ERK activation after H $_2$ O $_2$ treatment might be beneficial for the cells, results from PD98059 could not support this statement.

There is a possibility that the saving effect of AG126 is not related to ERK inhibition. Under the current experimental conditions, AG126 at 10 μ M was protective but it enhanced H $_2$ O $_2$ toxicity at 20 μ M. These results were consistent with those reported by Sagara et al. [52]. AG126 belongs to a group of tyrosine kinase inhibitors named tyrphostins. Many of these agents can prevent cellular oxidative stress including that generated by glutamate. There is no correlation between the kinase inhibition and the observed protective effect. Overnight treatment of cells with AG126 can increase cellular glutathione levels. Furthermore, this agent has some anti-oxidant effect based on the Trolox Equivalent Activity Concentration [52]. Collectively, this may explain the observation that AG126 at 10 μ M could partially prevent H $_2$ O $_2$ induced cytotoxicity. This agent can also function as a mitochondria uncou-

pler, thus it actually enhances H $_2$ O $_2$ cytotoxicity at higher concentrations [52].

An accumulation of 4-HNE-conjugated protein has been detected in lesions of aging-related diseases, including Parkinson's disease [53] and Alzheimer's disease [54]. It also accumulates in the affected neuronal tissues of experimental animals experiencing brain ischemia [55,56] and traumatic spinal cord injury [57]. 4-HNE can impair synaptosomal membrane proteins, glutamate transport and importantly, mitochondrial functions [58,59]. Evidence indicates that 4-HNE increases neuronal susceptibility to oxidative stress [60] and serves as a mediator of oxidative stress that leads to neuronal apoptosis [61]. As indicated in the Introduction, 4-HNE has been implicated in some ocular pathological conditions [19,20].

Several laboratories have attempted to document the formation of 4-HNE protein adducts during oxidative stress by Western blot analysis. Uchida et al. first reported oxidative stress caused by t-butylhydroperoxide or iron/ascorbate could lead to 4-HNE protein adducts in hepatocytes [62]. Further studies by these researchers attempted to identify the common epitope recognized by the 4-HNE antibodies. However, no specific protein was positively identified [63]. More recently, the formation of 4-HNE protein adducts was also demonstrated by Western blot analysis from the heart [64], the liver [65] and the kidney [66] under oxidative stress. It is important to point out that the patterns of 4-HNE protein adducts, as shown by these Western blot analyses, were different among these studies, probably as a result of tissue specificity. No particular protein was identified as a specific target for 4-HNE adduct formation in these studies. Results from the current study indicate that H $_2$ O $_2$ treatment of RPE could lead to the accumulation of 4-HNE protein adducts in the cytoplasm and the nuclei of these cells (Fig. 3). There was a dose-dependent increase of 4-HNE protein adduct after H $_2$ O $_2$ treatment with a maximal intensity of \sim 7X control at 2 mM H $_2$ O $_2$ (Fig. 3C). This may partially contribute to oxidative stress induced ocular disease. Even though ocular tissues, including the retina, contain glutathione S-transferases that can actively detoxify 4-HNE [35,67], adverse events may occur if aging or pathological conditions hinder this normal defense from functioning properly. It warrants further studies to identify those proteins species that are modified by 4-HNE.

Conclusions

This study demonstrates that oxidative stress induced by H $_2$ O $_2$ could lead to RPE cell death, which is preceded by distinct morphological changes, ERK activation and 4-HNE protein adduct formation. The cell death can be prevented partially by AG126, and the prostaglandin derivative, 15d-PGJ $_2$. These agents may be useful

pharmacological tools in the future capable of preventing oxidative stress induced RPE cell death in human ocular diseases.

Competing Interests

None declared.

Authors' Contributions

TKG and JYC were both involved in the experimental design and data collection. Both authors read and approved the final manuscript.

Abbreviations

15d-PG₂, 15-deoxy-delta 12, 14-Prostaglandin J₂; ERK, Extracellular signal-Regulated Kinase; 4-HNE, 4-hydroxynonenal, MAP kinases, Mitogen-Activated Protein kinases; MTT (3-(4,5-dimethylthiazol-2-yl)-2,5-diphenyltetrazolium bromide); PBS, phosphate-buffered saline; PPARs, peroxisome proliferator-activated receptors; RPE, retinal pigment epithelium.

Acknowledgments

This work was supported by funds from Fight For Sight and Research to Prevent Blindness. Primary human RPE cell cultures were prepared from specimens provided by the Arkansas Lions Eye Bank & Laboratory. Support by the Pat & Williard Walker Eye Research Center is greatly appreciated.

References

1. Rozanowska M, Jarvis-Evans J, Korytowski W, Boulton ME, Burke JM and Sarna T **Blue light-induced reactivity of retinal age pigment. In vitro generation of oxygen-reactive species** *J. Biol. Chem.* 1995, **270**:18825-18830
2. Miceli MV, Liles MR and Newsome DA **Evaluation of oxidative processes in human pigment epithelial cells associated with retinal outer segment phagocytosis** *Exp. Cell Res.* 1994, **214**:242-249
3. Tate DJ, Jr., Miceli MV and Newsome DA **Phagocytosis and H₂O₂ induce catalase and metallothionein gene expression in human retinal pigment epithelial cells** *Invest. Ophthalmol. Vis. Sci.* 1995, **36**:1271-1279
4. Cai J, Nelson KC, Wu M, Sternberg P, Jr. and Jones DP **Oxidative damage and protection of the RPE** *Prog. Retin. Eye Res.* 2000, **19**:205-221
5. Winkler BS, Boulton ME, Gottsch JD and Sternberg P **Oxidative damage and age-related macular degeneration** *Mol. Vis.* 1999, **5**:32-42
6. Wills NK, Weng T, Mo L, Hellmich HL, Yu A, Wang T, Buchheit S and Godley BF **Chloride channel expression in cultured human fetal RPE cells: response to oxidative stress** *Invest. Ophthalmol. Vis. Sci.* 2000, **41**:4247-4255
7. Jahngen-Hodge J, Obin MS, Gong X, Shang F, Nowell T.R., Jr., Gong J, Abasi H, Blumberg J and Taylor A **Regulation of ubiquitin-conjugating enzymes by glutathione following oxidative stress** *J. Biol. Chem.* 1997, **272**:28218-28226
8. Barak A, Morse LS and Goldkorn T **Ceramide: a potential mediator of apoptosis in human retinal pigment epithelial cells** *Invest. Ophthalmol. Vis. Sci.* 2001, **42**:247-254
9. Tate DJ, Miceli MV and Newsome DA **Zinc protects against oxidative damage in cultured human retinal pigment epithelial cells** *Free Radic. Biol. Med.* 1999, **26**:704-713
10. Ballinger SW, Van Houten B, Jin GF, Conklin CA and Godley BF **Hydrogen peroxide causes significant mitochondrial DNA damage in human RPE cells** *Exp. Eye Res.* 1999, **68**:765-772
11. Verna LK, Holman SA, Lee VC and Hoh J **UVA-induced oxidative damage in retinal pigment epithelial cells after H₂O₂ or sparflaxacin exposure** *Cell. Biol. Toxicol.* 2000, **16**:303-312
12. Jin GF, Hurst JS and Godley BF **Hydrogen peroxide stimulates apoptosis in cultured human retinal pigment epithelial cells** *Curr Eye Res.* 2001, **22**:165-173
13. Dalle-Donne I, Rossi R, Milzani A, Di Simplicio P and Colombo R **The actin cytoskeleton response to oxidants: from small heat shock protein phosphorylation to changes in the redox state of actin itself** *Free Radic. Biol. Med.* 2001, **31**:1624-1632
14. Bhat NR and Zhang P **Hydrogen peroxide activation of multiple mitogen-activated protein kinases in an oligodendrocyte cell line: role of extracellular signal-regulated kinase in hydrogen peroxide-induced cell death** *J. Neurochem.* 1999, **72**:112-119
15. Wang X, Martindale JL, Liu Y and Holbrook NJ **The cellular response to oxidative stress: influences of mitogen-activated protein kinase signalling pathways on cell survival** *Biochem. J.* 1998, **333**:291-300
16. Keller JN and Mattson MP **Roles of lipid peroxidation in modulation of cellular signaling pathways, cell dysfunction, and death in the nervous system** *Rev. Neurosci.* 1998, **9**:105-116
17. Verdejo C, Marco P, Renau-Piqueras J and Pinazo-Duran MD **Lipid peroxidation in proliferative vitreoretinopathies** *Eye* 1999, **13**:183-188
18. van Kuijk FJ **4-Hydroxynonenal interaction with rhodopsin** *Biochem. Biophys. Res. Commun.* 1997, **230**:275-279
19. Ansari NH, Wang L and Srivastava SK **Role of lipid aldehydes in cataractogenesis: 4-hydroxynonenal-induced cataract** *Biochem. Mol. Med.* 1996, **58**:25-30
20. Srivastava SK, Awasthi S, Wang L, Bhatnagar A, Awasthi YC and Ansari NH **Attenuation of 4-hydroxynonenal-induced cataractogenesis in rat lens by butylated hydroxytoluene** *Curr Eye Res.* 1996, **15**:749-754
21. Kersten S, Desvergne B and Wahli W **Roles of PPARs in health and disease** *Nature* 2000, **405**:421-424
22. Corton JC, Anderson SP and Stauber A **Central role of peroxisome proliferator-activated receptors in the actions of peroxisome proliferators** *Annu. Rev. Pharmacol. Toxicol.* 2000, **40**:491-518
23. Bishop-Bailey D **Peroxisome proliferator-activated receptors in the cardiovascular system** *Br. J. Pharmacol.* 2000, **129**:823-834
24. Ershov AV and Bazan NG **Photoreceptor phagocytosis selectively activates PPARgamma expression in retinal pigment epithelial cells** *J. Neurosci. Res.* 2000, **60**:328-337
25. Dunn KC, Aotaki-Keen AE, Putkey FR and Hjelmeland LM **ARPE-19, a human retinal pigment epithelial cell line with differentiated properties** *Exp. Eye Res.* 1996, **62**:155-169
26. Dunn KC, Marmorstein AD, Bonilha VL, Rodriguez-Boulant E, Giordano F and Hjelmeland LM **Use of the ARPE-19 cell line as a model of RPE polarity: basolateral secretion of FGF5** *Invest. Ophthalmol. Vis. Sci.* 1998, **39**:2744-2749
27. Chang JY and Liu L **Peroxisome proliferator-activated receptor agonists prevent 25-OH-cholesterol induced c-jun activation and cell death** *BMC Pharmacol.* 2001, **1**:10
28. Carter CA, Parham GP and Chambers T **Cytoskeletal reorganization induced by retinoic acid treatment of human endometrial adenocarcinoma (RL95-2) cells is correlated with alterations in protein kinase C-alpha** *Pathobiology* 1998, **66**:284-292
29. Wada M, Gelfman CM, Matsunaga H, Alizadeh M, Morse L, Handa JT and Hjelmeland LM **Density-dependent expression of FGF-2 in response to oxidative stress in RPE cells in vitro** *Curr. Eye Res.* 2001, **23**:226-231
30. Willson TM, Cobb JE, Cowan DJ, Wiethe RW, Correa ID, Prakash SR, Beck KD, Moore LB, Kliever SA and Lehmann JM **The structure-activity relationship between peroxisome proliferator-activated receptor gamma agonism and the antihyperglycemic activity of thiazolidinediones** *J. Med. Chem.* 1996, **39**:665-668
31. Davies SS, Pontsler AV, Marathe GK, Harrison KA, Murphy RC, Hinchaw JC, Prestwich GD, Hilaire AS, Prescott SM, Zimmerman GA and McIntyre TM **Oxidized alkyl phospholipids are specific, high affinity peroxisome proliferator-activated receptor gamma ligands and agonists** *J. Biol. Chem.* 2001, **276**:16015-16023
32. Kliever SA, Forman BM, Blumberg B, Ong ES, Borgmeyer U, Mangelsdorf DJ, Umesono K and Evans RM **Differential expression and activation of a family of murine peroxisome proliferator-activated receptors** *Proc. Natl. Acad. Sci. U.S.A.* 1994, **91**:7355-7359

33. Pang L, Sawada T, Decker SJ and Saltiel AR **Inhibition of MAP kinase blocks the differentiation of PC-12 cells induced by nerve growth factor** *J. Biol. Chem.* 1995, **270**:13585-13588
34. Levitzki A and Gazit A **Tyrosine kinase inhibition: an approach to drug development** *Science* 1995, **267**:1782-1788
35. Singhal SS, Godley BF, Chandra A, Pandya U, Jin GF, Saini MK, Awasthi S and Awasthi YC **Induction of glutathione S-transferase hGST 5.8 is an early response to oxidative stress in RPE cells** *Invest. Ophthalmol. Vis. Sci.* 1999, **40**:2652-2659
36. Tate DJ, Newsome DA and Oliver PD **Metallothionein shows an age-related decrease in human macular retinal pigment epithelium** *Invest. Ophthalmol. Vis. Sci.* 1993, **34**:2348-2351
37. Liles MR, Newsome DA and Oliver PD **Antioxidant enzymes in the aging human retinal pigment epithelium** *Arch. Ophthalmol.* 1991, **109**:1285-1288
38. Zhao Y and Davis HW **Hydrogen peroxide-induced cytoskeletal rearrangement in cultured pulmonary endothelial cells** *J. Cell. Physiol.* 1998, **174**:370-379
39. Liu SM and Sundqvist T **Nitric oxide and cGMP regulate endothelial permeability and F-actin distribution in hydrogen peroxide-treated endothelial cells** *Exp. Cell Res.* 1997, **235**:238-244
40. Adams JC **Formation of stable microspikes containing actin and the 55 kDa actin bundling protein, fascin, is a consequence of cell adhesion to thrombospondin-1: implications for the anti-adhesive activities of thrombospondin-1** *J. Cell Sci.* 1995, **108** (Pt 5):1977-1990
41. Huot J, Houle F, Rousseau S, Deschesnes RG, Shah GM and Landry J **SAPK2/p38-dependent F-actin reorganization regulates early membrane blebbing during stress-induced apoptosis** *J. Cell Biol.* 1998, **143**:1361-1373
42. O'Connell SR and Bressler NM **Age-related macular degeneration** *Vitreoretinal disease: The essentials* (Edited by: Regillo CD, Brown GC and Flynn HW Jr) New York, Thieme Medical Publishers, Inc. 1999, 213-240
43. Murata T, He S, Hangai M, Ishibashi T, Xi XP, Kim S, Hsueh WA, Ryan SJ, Law RE and Hinton DR **Peroxisome proliferator-activated receptor-gamma ligands inhibit choroidal neovascularization** *Invest. Ophthalmol. Vis. Sci.* 2000, **41**:2309-2317
44. Vaidya S, Somers EP, Wright SD, Detmers PA and Bansal VS **15-Deoxy-Delta12,1412,14-prostaglandin J2 inhibits the beta2 integrin-dependent oxidative burst: involvement of a mechanism distinct from peroxisome proliferator-activated receptor gamma ligation** *J. Immunol.* 1999, **163**:6187-6192
45. Ward C, Dransfield I, Murray J, Farrow SN, Haslett C and Rossi AG **Prostaglandin D2 and its metabolites induce caspase-dependent granulocyte apoptosis that is mediated via inhibition of I kappa B alpha degradation using a peroxisome proliferator-activated receptor-gamma-independent mechanism** *J. Immunol.* 2002, **168**:6232-6243
46. Jozkowicz A, Dulak J, Prager M, Nanobashvili J, Nigisch A, Winter B, Weigel G and Huk I **Prostaglandin-J2 induces synthesis of interleukin-8 by endothelial cells in a PPAR-gamma-independent manner** *Prostaglandins Other Lipid Mediat.* 2001, **66**:165-177
47. Bernardo A, Levi G and Minghetti L **Role of the peroxisome proliferator-activated receptor-gamma (PPAR-gamma) and its natural ligand 15-deoxy-Delta12, 14-prostaglandin J2 in the regulation of microglial functions** *Eur. J. Neurosci.* 2000, **12**:2215-2223
48. Petrova TV, Akama KT and Van Eldik LJ **Cyclopentenone prostaglandins suppress activation of microglia: down-regulation of inducible nitric-oxide synthase by 15-deoxy-Delta12,14-prostaglandin J2** *Proc. Natl. Acad. Sci. USA* 1999, **96**:4668-4673
49. Drew PD and Chavis JA **The cyclopentenone prostaglandin 15-deoxy-Delta(12,14) prostaglandin J2 represses nitric oxide, TNF-alpha, and IL-12 production by microglial cells** *J. Neuroimmunol.* 2001, **115**:28-35
50. Diab A, Deng C, Smith JD, Hussain RZ, Phanavanh B, Lovett-Racke AE, Drew PD and Racke MK **Peroxisome proliferator-activated receptor-gamma agonist 15-deoxy-Delta(12,14)-prostaglandin J(2) ameliorates experimental autoimmune encephalomyelitis** *J. Immunol.* 2002, **168**:2508-2515
51. Yoshizumi M, Abe J, Haendeler J, Huang Q and Berk BC **Src and Cas mediate JNK activation but not ERK1/2 and p38 kinases by reactive oxygen species** *J. Biol. Chem.* 2000, **275**:11706-11712
52. Sagara Y, Ishige K, Tsai C and Maher P **Tyrphostins protect neuronal cells from oxidative stress** *J. Biol. Chem.* 2002, **277**:36204-36215
53. Yoritaka A, Hattori N, Uchida K, Tanaka M, Stadtman ER and Mizuno Y **Immunohistochemical detection of 4-hydroxynonenal protein adducts in Parkinson disease** *Proc. Natl. Acad. Sci. USA* 1996, **93**:2696-2701
54. Takeda A, Smith MA, Avila J, Nunomura A, Siedlak SL, Zhu X, Perry G and Sayre LM **In Alzheimer's disease, heme oxygenase is coincident with Alz50, an epitope of tau induced by 4-hydroxy-2-nonenal modification** *J. Neurochem.* 2000, **75**:1234-1241
55. Urabe T, Yamasaki Y, Hattori N, Yoshikawa M, Uchida K and Mizuno Y **Accumulation of 4-hydroxynonenal-modified proteins in hippocampal CA1 pyramidal neurons precedes delayed neuronal damage in the gerbil brain** *Neuroscience* 2000, **100**:241-250
56. Yoshino H, Hattori N, Urabe T, Uchida K, Tanaka M and Mizuno Y **Postischemic accumulation of lipid peroxidation products in the rat brain: immunohistochemical detection of 4-hydroxy-2-nonenal modified proteins** *Brain Res.* 1997, **767**:81-86
57. Springer JE, Azbill RD, Mark RJ, Begley JG, Waeg G and Mattson MP **4-hydroxynonenal, a lipid peroxidation product, rapidly accumulates following traumatic spinal cord injury and inhibits glutamate uptake** *J. Neurochem.* 1997, **68**:2469-2476
58. Keller JN, Mark RJ, Bruce AJ, Blanc E, Rothstein JD, Uchida K, Waeg G and Mattson MP **4-Hydroxynonenal, an aldehydic product of membrane lipid peroxidation, impairs glutamate transport and mitochondrial function in synaptosomes** *Neuroscience* 1997, **80**:685-696
59. Subramaniam R, Roediger F, Jordan B, Mattson MP, Keller JN, Waeg G and Butterfield DA **The lipid peroxidation product, 4-hydroxy-2-trans-nonenal, alters the conformation of cortical synaptosomal membrane proteins** *J. Neurochem.* 1997, **69**:1161-1169
60. Keller JN, Hanni KB and Markesbery WR **4-hydroxynonenal increases neuronal susceptibility to oxidative stress** *J. Neurosci. Res.* 1999, **58**:823-830
61. Kruman I, Bruce-Keller AJ, Bredesen D, Waeg G and Mattson MP **Evidence that 4-hydroxynonenal mediates oxidative stress-induced neuronal apoptosis** *J. Neurosci.* 1997, **17**:5089-5100
62. Uchida K, Szweda LI, Chae HZ and Stadtman ER **Immunochemical detection of 4-hydroxynonenal protein adducts in oxidized hepatocytes** *Proc. Natl. Acad. Sci. U.S.A* 1993, **90**:8742-8746
63. Uchida K, Itakura K, Kawakishi S, Hiai H, Toyokuni S and Stadtman ER **Characterization of epitopes recognized by 4-hydroxy-2-nonenal specific antibodies** *Arch. Biochem. Biophys.* 1995, **324**:241-248
64. Eaton P, Li JM, Hearse DJ and Shattock MJ **Formation of 4-hydroxy-2-nonenal-modified proteins in ischemic rat heart** *Am. J. Physiol.* 1999, **276**:H935-NaN
65. Zhang C, Walker LM, Hinson JA and Mayeux PR **Oxidant stress in rat liver after lipopolysaccharide administration: effect of inducible nitric-oxide synthase inhibition** *J. Pharmacol. Exp. Ther.* 2000, **293**:968-972
66. Walker LM, York JL, Imam SZ, Ali SF, Muldrew KL and Mayeux PR **Oxidative stress and reactive nitrogen species generation during renal ischemia** *Toxicol. Sci.* 2001, **63**:143-148
67. Singhal SS, Awasthi S, Srivastava SK, Zimniak P, Ansari NH and Awasthi YC **Novel human ocular glutathione S-transferases with high activity toward 4-hydroxynonenal** *Invest. Ophthalmol. Vis. Sci.* 1995, **36**:142-150

Pre-publication history

The pre-publication history for this paper can be accessed here:

<http://www.biomedcentral.com/1471-2415/3/5/prepub>